ELSEVIER

Applied Surface Science 193 (2002) 129–137

applied surface science

www.elsevier.com/locate/apsusc

Surface structure and field emission property of carbon nanotubes grown by radio-frequency plasma-enhanced chemical vapor deposition

Yeon Sik Jung, Duk Young Jeon*

Department of Materials Science and Engineering, Korea Advanced Institute of Science and Technology, 373-1, Kusong-dong, Yusung-gu, Taejon 305-701, South Korea

Received 6 March 2002; received in revised form 6 March 2002; accepted 26 March 2002

Abstract

In this study, large-area and low-temperature synthesis of carbon nanotubes on glass substrates with transformer coupled plasma (TCP) type radio-frequency plasma-enhanced chemical vapor deposition (rf PE-CVD) system was performed, and their surface structures and field emission property were analyzed. By varying process conditions such as Ni layer thickness, gas flow rate, NH_3 etching time, plasma power, and the distance between rf coil and substrate, the optimum conditions for growing carbon nanotubes were found. Their SEM and TEM images showed that their diameters are ranged from 40 to 80 nm, and they have hollow tube structures. From the FTIR spectrum of carbon nanotubes synthesized in this study, large amount of $–CH_2$ and $–CH_3$ functional groups were detected, and the XPS peak of C1s was split into one main peak and several small peaks, which means the chemical state of carbon atoms is divided.

Their surface structures were proposed from the FTIR spectrum and the XPS results, and they are somewhat different from the samples grown by arc-discharge. The measured field emission current density seems to be sufficient to be used for field emission display and increased with the growth time of carbon nanotubes. With these results and equivalent circuit modeling, body-emission was confirmed to be a dominant emission mechanism. © 2002 Elsevier Science B.V. All rights reserved.

PACS: 61.46.+w; Nanoscale materials; Clusters; Nanoparticles; Nanotubes; Nanocrystals

Keywords: Carbon nanotube; PE-CVD; FTIR; XPS; Field emission

1. Introduction

Carbon nanotubes (CNTs) have been called as ‘new material for the 21st century’ owing to their amazing electrical and mechanical characteristics [1–3]. They have various applications such as a tip material for field emission devices [4] and scanning probe microscopy [5], an intercalation material for Li ion battery [6], a storage material for hydrogen gas [7], and so on. But many technical problems remain also because it is not easy to control them due to their very small size. Moreover, to commercialize them would not become active, until the techniques for large-scale and low-cost synthesis are developed. Particularly, uniformity of field emission, large area synthesis, low temperature synthesis, reproducibility, and so on are important issues for CNT field emission array. In this paper, we report some advances in growth of CNTs with

* Corresponding author. Tel.: +82-42-869-3337; fax: +82-42-869-3310.
E-mail address: dyj@mail.kaist.ac.kr (D.Y. Jeon).

0169-4332/02/$ – see front matter © 2002 Elsevier Science B.V. All rights reserved.
PII: S0169-4332(02)00227-1

transformer coupled plasma (TCP) type radio-frequency plasma-enhanced chemical vapor deposition (rf PE-CVD) system.

Many kinds of characterizations on CNTs have been conducted [8,9], but the differences in surface characteristics of CNTs resulted from different synthesis methods have not been fully researched yet. So we tried more detailed characterizations using tools such as RAMAN, FTIR, and XPS. We have obtained quite different RAMAN spectrum of the CNTs grown by rf PE-CVD from that of arc-discharged samples. And the spectra of FTIR and XPS showed that many functional groups exist on the surface of CNTs produced by rf PE-CVD, but only small quantity does in the case of arc-discharged samples. Field emission property was also measured and sufficient current density for field emission displays was obtained. Some researchers have proposed body-emission mechanism [10], but they have not given satisfactory evidences yet. We shall present new evidences for body-emission mechanism and equivalent circuit models by comparing the field emission current densities of the CNT samples of different growth times.

2. Experiments

Experiments were composed of three parts, which were the synthesis of CNTs with rf PE-CVD system, structure analysis using analytical tools, and the measurements of field emission property.

Inductively coupled plasma (ICP), electron cyclotron resonance (ECR) plasma, and Helicon plasma are examples of high-density plasma for thin film deposition. TCP system that we selected is a planar type of ICP system. While a coil is wound like a helix along an alumina or quartz tube coil in an ICP system, a TCP system has a planar coil over a quartz plate for generating high-density plasma. We chose a TCP type rf PE-CVD system for the synthesis of CNTs because uniform and large-area deposition is possible at low temperature, and additional economic advantages for commercialization are provided owing to its simple structure.

As seen in Fig. 1, an rf coil is laid over the quartz plate. If time-varying magnetic waves are transferred to the gas in the chamber, time-varying electric field is induced and subsequently the accelerated electrons generate high-density plasma.

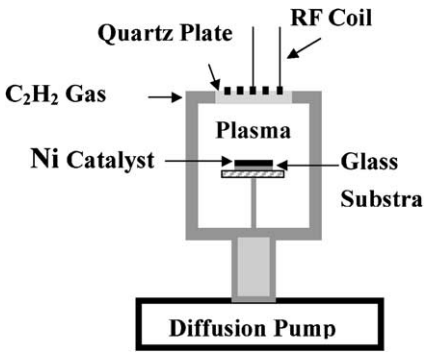

Fig. 1. Schematic diagram of TCP type rf plasma enhanced CVD system.

Ni catalysts of 100–300 Å thick were deposited on glass substrates by dc magnetron sputtering and the substrates were heated to 150 °C during deposition to increase their adhesion property. NH_3 plasma treatment on Ni surface was performed to form catalytic seed particles for the synthesis of CNTs. NH_3 flow rate was 10–300 sccm and treatment time was 0–240 min. With the Ni particles formed on glass substrates, the optimum conditions for growing dense and uniform CNTs were searched by varying process conditions. C_2H_2 flow rate was ranged from 10 to 200 sccm, rf power from 50 to 200 W, substrate temperature 450–550 °C, and the distance between the rf coil and substrates 10–50 cm.

To identify the optimum synthesis of CNTs, SEM and TEM analysis were done using Philips XL 30S FEG and EM 912 Omega (LEO) equipments, respectively. And U-1000 RAMAN system was used to characterize the vibrational properties of CNTs. MB154-BOMEM system and VG Scientific ESCA LAB 2000R equipments were also utilized for FTIR and XPS analysis. Finally, field emission measurements were conducted in a vacuum system under the pressure of 2.5×10^{-7} Torr and with the electrode gap of 150 μm.

3. Results and discussions

3.1. Synthesis of carbon nanotubes

To find out the optimum growth condition of CNTs, we analyzed SEM images while varying several process variables listed in Table 1. ‘O’ means that CNTs were grown and ‘X’ means CNTs were not grown. (Bold values mean better growth.)

Table 1
Best conditions for growing carbon nanotubes by rf PE-CVD

Process variables	Process conditions				
Ni thickness (Å)	100	150	**200**	250	300
	X	X	**O**	O	O
NH_3 flow rate (pretreatment) (sccm)	30	50	**100**	**200**	**300**
	O	O	**O**	**O**	**O**
NH_3 pretreatment time (for Ni 300 Å) (min)	30	60	**120**	**180**	240
	X	O	**O**	**O**	X
Substrate temperature (°C)	450	**500**	**550**		
	X	**O**	**O**		
C_2H_2 flow rate (sccm)	30	**50**	**100**	**150**	200
	X	**O**	**O**	**O**	X
Plasma power (W)	50	**100**	**150**	200	
	O	**O**	**O**	X	
Coil-substrate distance (cm)	**10**	20	40		
	O	X	X		

'O' means grown and 'X' means not grown and bold values indicate better growth.

Proper thickness of Ni catalysts for the growth of CNTs was found in the range of 200–300 Å. Suitable duration of NH_3 plasma etching process was varied depending upon the Ni thickness. For example, the Ni catalyst of 300 Å thick needed 180 min of NH_3 plasma treatment time. Treatment of over 240 min removed the Ni layer completely and CNTs were not synthesized. And the synthesis was successful when C_2H_2 gas was flown in the range of 50–150 sccm. That means an optimum pressure exists for the growth of CNTs. And an appropriate rf power was between 100 and 150 W. Finally, we ascertained that another important variable was the distance between the rf coil and the substrate. If the distance was over 20 cm, CNTs were not grown.

Fig. 2(a) shows the flat surface of an as-sputtered Ni sample. It is not suitable to be used as a catalyst for CNTs. It is well known that CNTs are not grown on such a smooth surface. After treated for 180 min with NH_3 plasma, the Ni seed particles of 20–30 nm were formed. The Ni particles were not so uniform because the Ni particles were not formed simultaneously and the particles formed earlier were etched away by the plasma (Fig. 2b). Much longer time was taken to form such particles than by dc PE-CVD system, and relatively lower process pressure (450 mTorr) seems to be the cause of it.

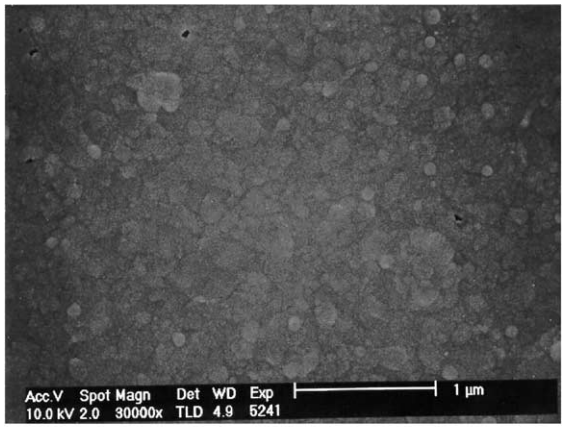

(a)

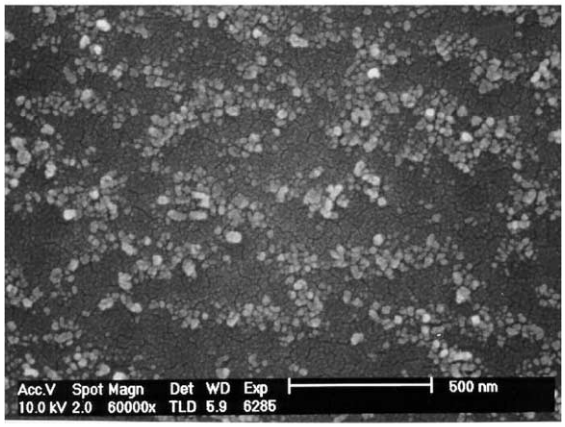

(b)

Fig. 2. Ni morphology change according to NH_3 treatment time (a) no treatment (b) 180 min.

After flowing C_2H_2 gas of 150 sccm and applying rf power of 100 W, dense CNTs were synthesized on that substrate. Fig. 3a and b shows the observed TEM image. The synthesized CNTs seemed to have hollow tube structure but some inclusions were found within the nanotubes having thick walls. The diameters of CNTs were ranged from 30 to 80 nm. And Ni catalytic particles were observed at the ends of the tubes.

3.2. Curved nanotubes

The previous results of many other researchers have shown that CNTs synthesized by arc-discharge are

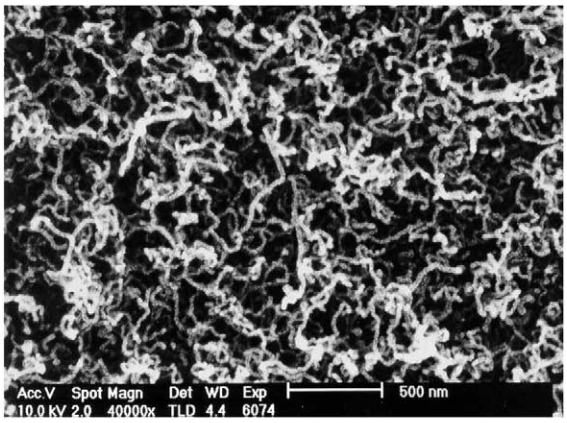

(a)

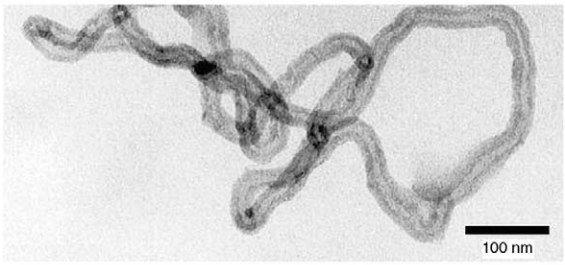

(b)

Fig. 3. (a) SEM and (b) TEM image of carbon nanotubes produced by rf PE-CVD.

very straight [11], but as seen in Fig. 3, the CNTs produced in this study seemed to be very twisty.

Amelinckx et al. proposed a growth mechanism for helical nanotubes in terms of active sites and extrusion velocity [12]. They explained that the locus of active site is circular and the extrusion velocity is kept constant during the growth process, in the case of straight nanotubes. On the other hand, catalytic activity varies periodically around the circumferences of helical CNTs during their growth process. Adopting their theory, we can expect that twisty CNTs are the results of very complex change of catalytic activity. Many researchers know from experience that the lower the process temperature is, the more curved the synthesized CNTs are. Now, the non-uniformity of temperature in the process chamber is thought to be the cause of their being twisty.

Generally, CVD processes are divided into two kinds of process region depending upon the rate determining steps. Relatively low temperature process is reaction rate limited and high temperature process is diffusion limited. We can easily distinguish the two regions by analyzing the graph of growth rate versus ($1/T$) (Arrhenius plot). The slope of low temperature region is much steeper than that of high temperature region. That means growth rate changes much more in low temperature process by a small fluctuation of temperature. The process temperature of this study was approximately 550 °C, which is relatively lower than in other researches using such as arc-discharge method, thermal CVD, or laser ablation. In practice, there are always some causes of temperature fluctuations in CVD chambers. They are large temperature gradient between substrate and chamber wall, the inflow of cold gases into the chamber, the generated heat by plasma and chemical reactions, and so on. The growth rate of graphitic layer will be much higher at the active site of larger catalytic activity (with slightly higher temperature) and that might be the cause of twisted CNTs in low temperature processes.

3.3. RAMAN measurements

Hiura et al. reported that first-order RAMAN spectra of CNTs produced by arc-discharge are characterized by a strong band at 1580 cm^{-1} and a very weak peak at 1350 cm^{-1} [8]. On the other hand, in the case of nanosoots (nanoparticles), Holdon et al. observed strong peaks at both 1580 and 1350 cm^{-1} [13]. These results have made the RAMAN technique as a good tool to characterize CNTs. The RAMAN spectrum of CNTs shown in Fig. 4 is quite different from that of CNTs produced by arc-discharge but very similar to that of nanosoots. Although they are uniform CNTs grown by rf PE-CVD, they have a strong band at 1350 cm^{-1} as well as at 1580 cm^{-1}. This result is consistent with Lee et al.'s measurements on CNTs grown by thermal CVD [9]. Then, it could be an inevitable question to answer why the RAMAN spectra of pure CNTs grown by CVD agree with those of nanosoots.

Nemanish et al. reported that smaller sizes of graphite crystallites (nanoparticles) result in stronger intensity of 1350 cm^{-1}, and Bacsa et al. explained that the peak at 1350 cm^{-1} is due to curved graphene sheets [14,15]. Here, it might be worth to notice that the CNTs produced in this study or in Lee's paper were

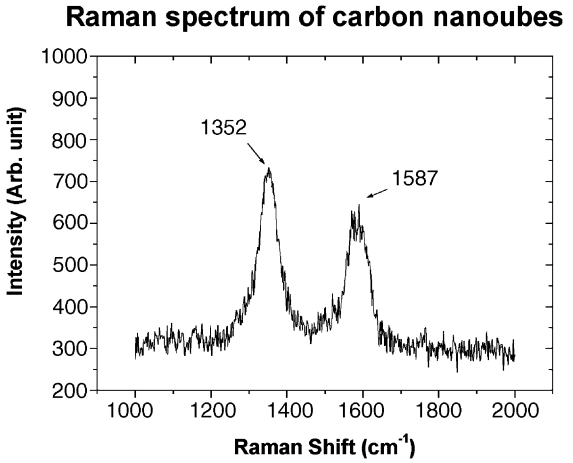

Fig. 4. Raman spectrum of carbon nanotubes synthesized by rf PE-CVD.

much twistier than those grown by arc-discharge. As illustrated in Fig. 5, curved graphen structure of a CNT (A) seems to be very analogous to that of a nanoparticles (B). Thus, unlike straight CNTs, curved parts of CNTs are expected to have RAMAN spectra very similar to those of nanosoots. More specifically, pentagon or heptagon defects contained in the curved parts of CNTs are thought to have resulted in so strong peak-intensity at 1350 cm^{-1}.

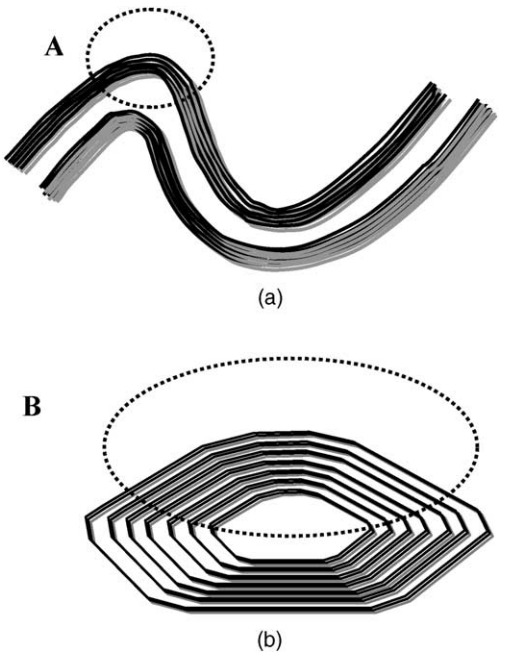

Fig. 5. Schematic diagram of (a) curved carbon nanotube and (b) carbon nanoparticle.

3.4. Surface characterization

The existence of seams in graphite layers observed by Chen et al. [10] made a question about the bonding state of carbon atoms in outer shells. It is curious to know whether the seams remain as dangling bonds, as they assumed, or form new bonds. They suggested that the seams with dangling bonds play a role in field emission. But the dangling bonds of much higher energy states are so unstable and CVD chambers using hydrocarbon precursors are full of hydrocarbon gases, radicals, and ions. Hence, we expected that functional group would saturate the dangling bonds. Fig. 6(a) shows the FTIR spectrum

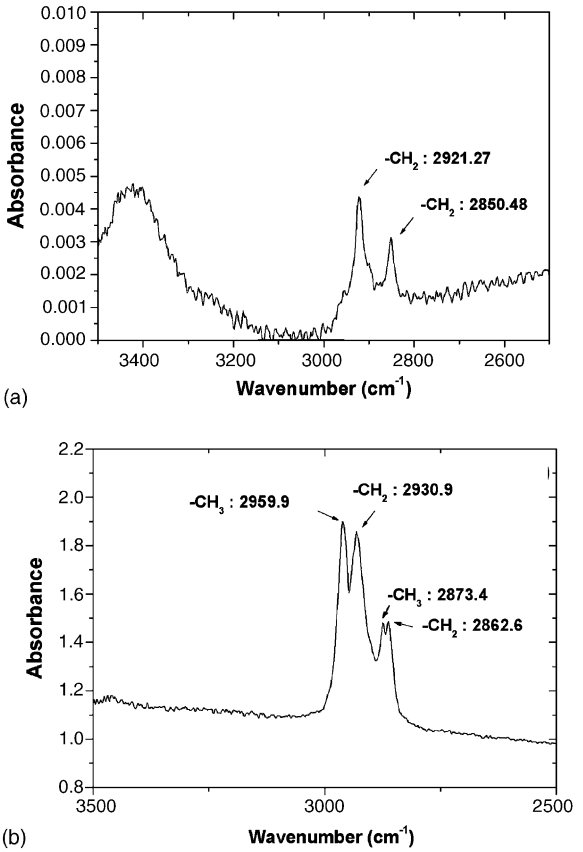

Fig. 6. FTIR spectra of carbon nanotubes produced by rf PE-CVD (a) arc-discharge (b) rf PE-CVD.

of CNTs synthesized by arc-discharge method where no hydrocarbon gas species are used. Only very small quantity of $–CH_2$ functional groups was detected at both 2921 and 2850.5 cm^{-1}. From the small peak intensity, the quantity seems to be very small, and they are thought to exist at the tips of the CNTs but we cannot deny the possibility of being dangled from the surface of nanoparticles. But the quantity is so small that they are beyond consideration.

On the contrary, Fig. 6(b) shows the strong peaks of the CNTs grown by rf PE-CVD at 2959 and 2930 cm^{-1} which correspond to asymmetric stretching vibration modes of $–CH_3$ and $–CH_2$, respectively. Because no peaks were observed beyond 3000 cm^{-1}, it seems that the functional groups are not alkenes or alkynes and they do not accompany double or triple bonds.

The peak intensities of $–CH_3$ and $–CH_2$ groups tell us more information. The peaks due to asymmetric stretching vibration have similar intensities, and the one at 2862.6 cm^{-1} (symmetric stretching vibration of $–CH_2$) has larger intensity than the one at 2873.4 cm^{-1} (symmetric stretching vibration of $–CH_2$), which appears so due to the influence of the peak at 2930 cm^{-1}.

In the meanwhile, the degeneracy of asymmetric stretching vibration by $–CH_3$ groups is 2, and 1 for $–CH_2$ groups. It means the peak intensity of asymmetric stretching vibration by $–CH_2$ groups is as much as half of $–CH_3$ groups if the numbers of the two kinds of functional groups are identical. So it is expected that more $–CH_2$ groups exist on the surface of CNTs grown by rf PE-CVD than $–CH_3$ groups do.

Fig. 7(a) shows the XPS results of the CNTs grown by arc-discharge. The graph is a narrow scan result for C 1s electron and is very similar to that of graphite carbon. It seems that the CNTs are composed of graphite layers of good crystallinity and do not contain any other bonding states such as C–H. But the C 1s peak of the CNTs grown by rf PE-CVD is divided into several small peaks, which means the bonding state of carbon atoms are split. The 284.5 eV peak corresponds to graphite carbon, and 284.9 and 285.7 eV are binding energy of 1s electrons of carbon atoms that have covalent bonds with hydrogen atoms. And the peaks at 284.2 and 284.0 eV are due to the hydrocarbon species absorbed on the Ni catalyst. In summary, the XPS data would be the indirect evidence for

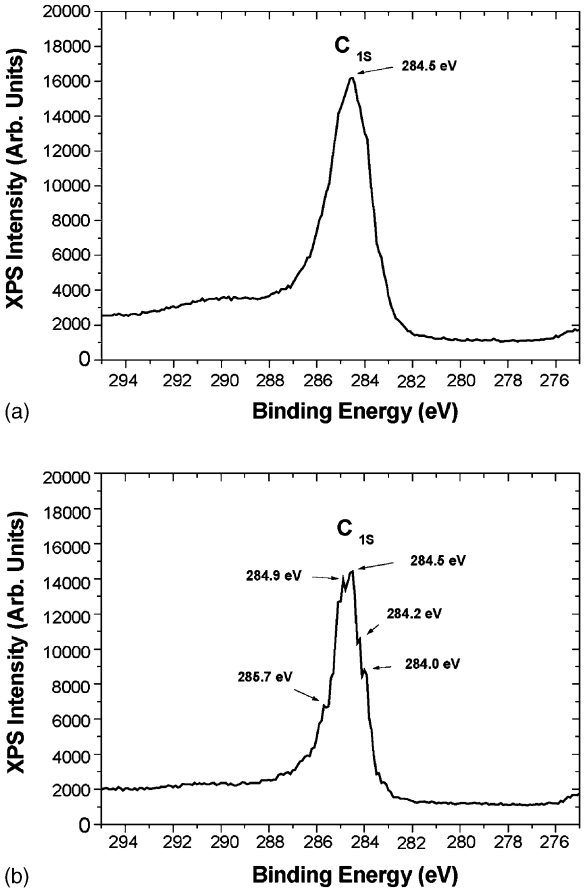

Fig. 7. XPS data of carbon nanotubes produced by (a) arc-discharge (b) rf PE-CVD.

the fact that some carbon atoms on the surface of CNTs grown by rf PE-CVD, are bonded with hydrocarbon species.

With the FTIR spectrum and XPS results, the surface structure of the CNTs grown by rf PE-CVD is proposed in Fig. 8. Different structures of A and B are illustrated to explain that the number of $–CH_2$ groups is more than that of $–CH_3$ groups. Combinational structures of A and B would be also possible.

3.5. Field emission measurements

Figs. 9 and 10 show the field emission properties of the CNTs with different growth times. Onset field was 3–4 V/μm and approximately 0.7 mA/cm^2 of current density at 4.5 V/μm was obtained in the case of the

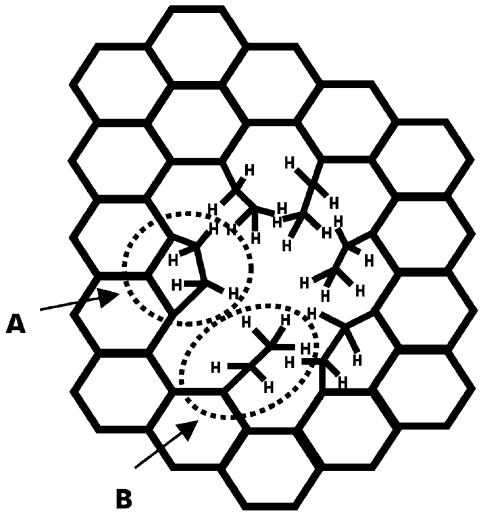

Fig. 8. Proposed surface structure of carbon nanotubes grown by rf PE-CVD.

samples of 30 and 50 min growth, and the value is known to be sufficient for flat panel displays.

Meanwhile, Chen et al. reported higher emission current density and lower onset voltage in the case of parallel alignment of CNTs than in the case of perpendicular alignment to substrates, and suggested a body-emission mechanism [10]. But the change in emission current density depending upon the orientation angle cannot be a sufficient evidence for the body-emission mechanism. It is because their result that the

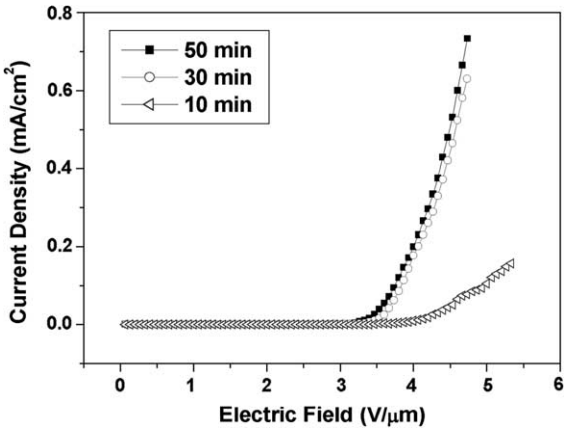

Fig. 9. Field emission curves depending upon carbon nanotube growth time.

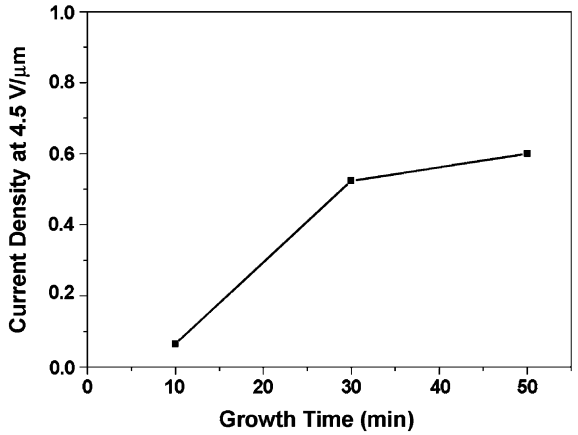

Fig. 10. Change in field emission current density depending upon carbon nanotubes growth time.

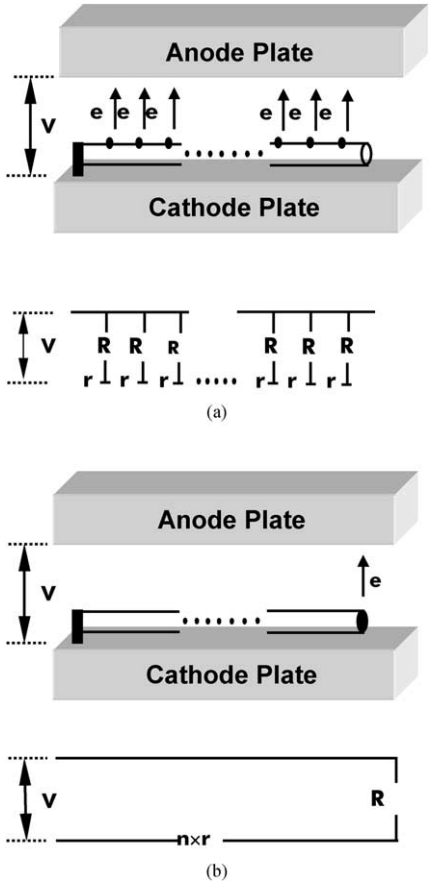

Fig. 11. Equivalent circuit model for field emission according to dominant emission mechanism (a) body-emission dominating case (b) tip-emission dominating case.

current density of a 45°-oriented sample was larger than that of a parallel sample could not be explained well. We think that the drastic increase of current density of the parallel sample was due to the increase of electrical contact area between CNTs and the cathode plate because they slid a Teflon rod on the 45°-oriented sample to fabricate the parallel sample. That process is thought to have lowered the contact resistance and the resulted decrease in voltage drop seems to be the cause of smaller onset field. So we compared the field emission curves of the CNTs of different growth times with each other to ascertain the body-emission mechanism. It was reported that the length of carbon nanotubes could be controlled by growth time, namely average length of CNTs increased with growth time [16]. The equivalent circuit models were suggested in Fig. 11 for (a) body-emission dominated case, and (b) tip-emission dominated case. On the basis of those models, the expected

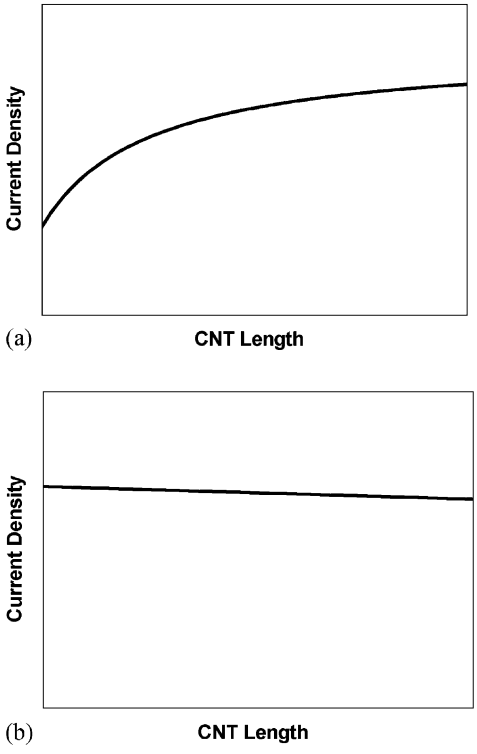

Fig. 12. Change in current density depending upon the length of a carbon nanotube in the case of two different emission mechanisms (a) body-emission dominating case (b) tip-emission dominating case.

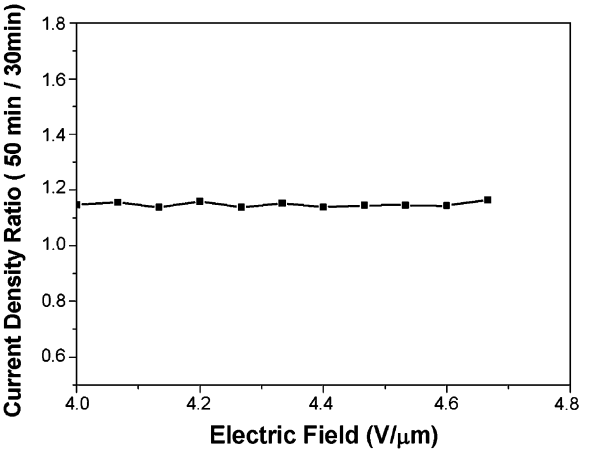

Fig. 13. Field emission current density ratio (50 min sample/30 min sample) as a function of electric field.

change in current density depending upon the length of CNTs are shown in Fig. 12(a) and (b). If the body-emission mechanism is dominant, then the number of emission sites would increase with the length of the CNTs and thus, the current density would increase. In tip-emission dominated case, however, the current density would be kept constant or slightly decreased due to increased resistance. Figs. 9 and 10 show that the emission current density increased with the growth time. In addition to that, Fig. 13 shows that the ratio of current densities (50 min sample/30 min sample) kept constant above the onset field. It means the number of emission sites kept at constant ratio, namely, the number of emission sites is proportional to the length of CNTs. This fact also supports body-emission mechanism.

These results seem to be good evidences for confirming the body-emission mechanism, and it explains well the impressive current density from randomly oriented CNT samples.

4. Conclusion

Dense arrays of carbon nanotubes were grown by TCP type rf PE-CVD on glass substrates of large area (3×3 cm) below 550 °C. SEM and TEM images show that their diameters are ranged from 40 to 80 nm and they have hollow tube structures. Graphitic layers were detected from RAMAN measurements.

Many $-CH_2$ and $-CH_3$ functional groups were detected from FTIR measurements. XPS peak of C 1s was split into one main peak and several small peaks. It means that the chemical state of carbon atoms is divided. Surface structure of carbon nanotubes synthesized in this work was proposed from the FTIR and the XPS measurements. Field emission current density was measured to be 0.7 mA/cm^2 at 4.5 V/μm and seems to be sufficient to be used for field emission display. Field emission current density increased with carbon nanotube growth time and body-emission was confirmed to be the dominant emission mechanism.

Acknowledgements

This work was supported by Center for Electronic Packaging Materials of Korea Science and Engineering Foundation.

References

[1] M.S. Dresselhaus, G. Dresselhaus, R. Saito, Carbon 33 (1995) 883.
[2] M.S. Dresselhaus, G. Dresselhaus, P.C. Eklund, Science of Fullerenes and Carbon Nanotubes, Academic Press, San Diego, 1996.
[3] M.M.J. Treacy, T.W. Ebbesen, J.M. Gibson, Nature 381 (1996) 678.
[4] W.A. de Heer, A. Chatelain, D. Ugarte et al., Science 270 (1995) 1179.
[5] H. Dai, J.H. Hafner, A.G. Rinzler, D.T. Colbert, R.E. Smalley, Nature 384 (1996) 147.
[6] T. Ishihara, A. Kawahara, H. Nishiguchi, M. Yoshio, Y. Takita, J. Power Sources 97 (1997) 192.
[7] N. Rajalakshmi, K.S. Dhathathreyan, A. Govindaraj, B.C. Satishkumar, Electrochim. Acta 45 (2000) 4511.
[8] H. Hiura, T.W. Ebbesen, K. Tanigaki, H. Takahashi, Chem. Phys. Lett. 202 (1993) 509.
[9] C.J. Lee, D.W. Kim, T.J. Lee, Y.C. Choi, Y.S. Park, W.S. Kim, W.B. Choi, N.S. Lee, J.M. Kim, Y.G. Choi, S.C. Yu, Y.H. Lee, Appl. Phys. Lett. 75 (1999) 1721.
[10] Y. Chen, D.T. Shaw, L. Guo, Appl. Phys. Lett. 76 (2000) 2469.
[11] T.W. Ebbesen, P.M. Ajayan, Nature 358 (1992) 220.
[12] S. Amelinckx, X.B. Zhang, D. Bernaerts, X.F. Zhang, V. Ivanov, J.B. Nagy, Science 265 (1994) 635.
[13] J.M. Holdon, P. Zhou, X. Bi, P.C. Eklund, S. Bandow, R.A. Jishi, K.D. Chowdhury, G. Dresselhaus, M.S. Dresselhaus, Chem. Phys. Lett. 200 (1994) 186.
[14] R.J. Nemanish, S.A. Solin, Phys. Rev. B 20 (1979) 392.
[15] W.S. Bacsa, D. Ugarte, A. Chatelain, W.A. De Heer, Chem. Phys. Lett. 211 (1993) 346.
[16] J.S. Suh, J.S. Lee, Appl. Phys. Lett. 75 (1999) 2047.